Article

Discovering a Dihydrofluorescein Analogue as a Promising Fluorescence Substrate to HRP

Jiayan Zhu [1], Ting Li [2], Shihui Zhang [2], Xiaomei Zou [1], Yingchun Zhou [1,*], Weiguo Lu [1], Zhihui Liu [1], Tao Deng [2,*] and Fang Liu [3,*]

[1] The First Clinical Medical College and the First Affiliated Hospital of Guangzhou University of Chinese Medicine, Guangzhou 510006, China
[2] Artemisinin Research Center, Guangzhou University of Chinese Medicine, Guangzhou 510006, China
[3] School of Pharmaceutical Sciences, Guangzhou University of Chinese Medicine, Guangzhou 510006, China
* Correspondence: yingchunbaby@126.com (Y.Z.); dengtao@gzucm.edu.cn (T.D.); fangliu@gzucm.edu.cn (F.L.)

Abstract: Horseradish peroxidase (HRP) combined with its fluorescence substrates is attracting increasing attention for biochemical analysis. Amplex red is the most widely used fluorescence substrate to HRP; however, it suffers from some drawbacks, such as nonspecific responsiveness toward carboxylesterases. Discovering a new small molecular fluorescence substrate with improved sensitivity and selectivity for HRP is thus desired. Herein, three dihydrofluorescein derivatives (DCFHs) are presented to serve as HRP substrates through fluorescence turn-on methods. The most promising one, 2,7-dichloro-9-(2-(hydroxymethyl)phenyl)-9H-xanthene-3,6-diol (**DCFH-1**), exhibited excellent sensitivity in the detection of HRP. Moreover, **DCFH-1** does not respond to carboxylesterase, thus holding advantages over Amplex red. In the further study, the detection reagent in the commercial ELISA kits was replaced with **DCFH-1** to establish a new fluorescence ELISA, which works very well in the quantification of inflammatory cytokine biomarkers from in vitro models.

Keywords: horseradish peroxidase (HRP); fluorescence substrate to HRP; dichlorodihydrofluorescein (DCFH); ELISA; fluorescence immunoassay

1. Introduction

HRP is a well-known peroxidase that can catalyze the oxidation of numerous small molecular substrates using H_2O_2 as the oxidant [1]. On this basis, the HRP/H_2O_2 system has been widely applied to generate optical signals during biochemical detection through oxidizing a proper chemical substrate. For example, HRP has been used to link with antibodies, which has been extensively used in immunoassays, including enzyme-linked immunosorbent assay (ELISA) and western blot (WB) [2–4]. HRP has also been used in multi-enzyme cascade reaction for the analysis of H_2O_2-generating systems [5,6]. The most commonly used HRP substrates can be categorized into three types: colorimetric, fluorometric and chemiluminescent. TMB (3,3′,5,5″-tetramethylbenzidine), Amplex red (10-acetyl-3,7-dihydroxyphenoxazine), and luminol (3-aminophthalhydrazide) are the most representative HRP substrates accordingly [7–9]. Among them, luminescent assay using HRP/luminol holds the greatest sensitivity, but chemiluminescence usually decays so fast that it can lead to difficulties in signal capturing and reproducing [10,11]. HRP/colorimetric substrates are the most popular due to their relatively lower equipment requirement. However, colorimetric assays often suffer from lower sensitivities when compared with luminescent and fluorescent assays [12–17]. HRP-based fluorescence assays are customarily characterized by the fluorescence changes upon detection, which is attracting increasing interest due to its relatively higher sensitivity and greater signal stability. Amplex red, also known as ADHP, is a highly sensitive fluorescence substrate of HRP, which has been utilized in most of the fluorescence ELISA kits in the market. Previous studies have indicated some drawbacks in the specificity of the HRP/Amplex Red reaction [9,18–21]. For example,

Satomi Miwa et al. found that carboxylesterase can convert Amplex red to the fluorescent product resorufin, thus leading to inaccuracy in the measurement of H_2O_2 from living cells and tissue/cell lysates with carboxylesterase expression [19,20]. Searching for the next generation HRP fluorescence substrates with excellent sensitivity and improved selectivity continually encouraged researchers in the last decade. Currently, there are several newly developed fluorescence substrates for HRP; some of them are based on fluorescence turn-off methods [22–25], and some are of fluorescence turn-on methods [26–31]. For example, Abhinav P. Acharya et al. prepared two hydrocyanine dyes that showed elevated detection sensitivity compared with TMB-based colorimetric assay [30]. Most recently, Liu, Jinhua et.al proposed an HRP/H_2O_2-mediated reaction between polyethyleneimine (PEI) and *p*-phenylenediamine (PPD), which can subsequently generate copolymer nanoparticles with green fluorescence. This method has been successfully used in sensitively detecting SARS-CoV-2 N protein through fluorescence ELISA [27]. Although some of the reported substrates have shown greater sensitivity than colorimetric assays, there is still a lack of direct comparison with the most commonly used fluorescence substrate, Amplex red.

Herein, three 2′,7′-dichlorodihydrofluorescein analogues (**DCFH-1** to **DCFH-3**) were prepared for a fluorescence-sensing HRP/H_2O_2 reaction. **DCFH-1** exhibits great potential to serve as a fluorescence turn-on HRP substrate. Fluorescence sensing HRP/H_2O_2 by **DCFH-1** was directly compared with the detection by Amplex red. Nonspecific reaction between carboxylesterase and **DCFH-1** was examined and the result was compared with that of Amplex red. In addition, **DCFH-1**-based fluorescence ELISA was successfully applied for the detection of cytokines from living cell cultures. The experimental details are described and discussed.

2. Experimental Method

2.1. Synthesis and Characterization

The targeted dichlorodihydrofluorescein analogues **DCFH-1** to **DCFH-3** were synthesized according to a mild synthetic procedure using 2,7-dichlorofluorescein (DCF) as the starting compound, where $NaBH_4$ was applied as the reduction reagent (Scheme 1 and Supplementary Materials). Briefly, for **DCFH-1** synthesis, $NaBH_4$ (6 mMol, 226.98 mg) was added portion-wise to the THF solution (4 mL) of DCF (1 mMol, 401.2 mg) at rt. When the gas evolution stopped, I_2 (3 mMol, 761.4 mg) was added slowly, and the reaction mixture was then heated to 60 °C in the dark. After 48 h reaction at 60 °C, the mixture was cooled to rt, followed by quenching with $Na_2S_2O_3 \cdot 5H_2O$ and saturated $NaHCO_3$ solution. The pH of the mixture was then adjusted to pH 5.0 using 2 M acetic acid, the aqueous layer was extracted with ethyl acetate (4 × 30 mL), the combined organic phase was washed with saturated NaCl, dried over Na_2SO_4 and concentrated under reduced pressure. The residue was purified by silica gel column chromatography (methanol: dichloromethane = 1:90) to give **DCFH-1** as a white solid (310 mg, 80% yield). ^1H nMR (400 MHz, DMSO-d_6) δ 10.43 (s, 2H), 7.38 (m, *J* = 5.7, 3.5 Hz, 1H), 7.17 (m, *J* = 5.7, 3.4 Hz, 2H), 6.95 (s, 3H), 6.72 (s, 2H), 5.53 (s, 1H), 5.40 (m, *J* = 5.2 Hz, 1H), 4.63 (d, *J* = 4.2 Hz, 2H). ^{13}C nMR (100 MHz, DMSO-d_6) δ 152.88, 149.51, 145.60, 138.93, 130.51, 130.46, 129.06, 128.58, 126.85, 116.42, 115.13, 104.13, 61.81, 37.32. HRMS (ESI) *m/z* calcd for $C_{20}H_{14}Cl_2O_4$ [M + Na]$^+$ 411.0161, found 411.0158.

The syntheses and characterization of **DCFH-2** and **DCFH-3** are detailed in the Supplementary Materials. I_2 was not needed for the reduction procedures of **DCFH-2** and **DCFH-3**.
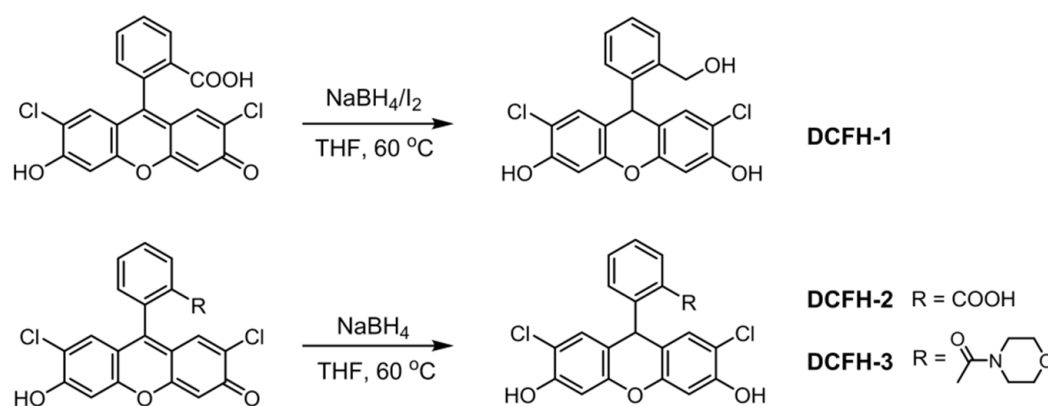
Scheme 1. The reduction procedure in the preparation of the targeted DCFHs.

2.2. Kinetic and Spectroscopy Measurement

PBS buffer (10 mM, pH 7.4) was used thoroughly for the measurement. Fluorescence substrate, H_2O_2 and HRP were dissolved in PBS buffer to prepare the corresponding solutions. For a typical test, fluorescence substrate was mixed with HRP first, followed by the addition of H_2O_2. Fluorescence intensity was collected by a multi-function plate reader. The fluorescence intensity at 586 nM of the Amplex red reaction solution was measured under 565 nM excitation. For **DCFH-1** reaction, fluorescence intensity at 528 nM was recorded upon 504 nM excitation. To collect the full fluorescence spectra, **DCFH-1** and Amplex red were excited at 450 nM and 520 nM, respectively.

2.3. Examination of the Reactivity of DCFH-1 and Amplex Red toward Carboxylesterase

For the test with the pure commercialized enzyme, 0.5 U/mL carboxylesterase was incubated with Amplex red or **DCFH-1** (both at 50 μM). The fluorescence intensity changes for **DCFH-1** (λ_{em} = 528 nM, λ_{ex} = 504 nM) and Amplex red (λ_{em} = 586 nM, λ_{ex} = 565 nM) were recorded by a plater reader. Phenylmethanesulfonyl fluoride (PMSF) was used as a nonspecific inhibitor to suppress the activity of carboxylesterase, whose final concentration was set at 100 μM. For the test with the esterase from living tissue samples, 100 mg fresh mouse liver tissue and one steel ball (4 mM diameter) were immersed in 1 mL PBS (pH 7.4), the tissue was then homogenized by an automatic homogenizer, followed by centrifugation at 1200 r/min for 4 min at 4 °C. The fresh supernatant was collected for use. The total protein in the supernatant was quantified by a standard BCA kit. The tissue extracts corresponding to 500 μg/mL protein were incubated with **DCFH-1** and Amplex red separately, and the fluorescence intensity changes were monitored by a plater reader.

2.4. Fluorescence ELISA Using DCFH-1 as HRP Substrate

Commercial ELISA kits for mouse tumor necrosis factor alpha (TNF-α, Cat. No: SEKM-0034, Solarbio, Beijing, China) and mouse interleukin 6 (IL-6, Cat. No: SEKM-0007, Solarbio, Beijing, China) were used for the test. TMB substrate supplied with the kits for detection were replaced by **DCFH-1** (100 μM in PBS 7.4). The H_2O_2 solution in the kit was also replaced with a newly prepared H_2O_2 solution (1 mM in PBS 7.4). **DCFH-1** was mixed with H_2O_2 at the volume ratio of 1:1 for later detection use. The analysis of TNF-α and IL-6 from the cell culture medium was according to the standard instruction supplied with the ELISA kits. Finally, the wells were incubated with the mixed **DCFH-1**/H_2O_2 solution for 20 min at rt, and fluorescence intensity at 528 nM upon 504 nM excitation was collected by a plate reader. A standard calibration curve for each cytokine was prepared using the ELISA kit supplied with **DCFH-1**. For the measurement over the highest concentration of the linear range, additional dilutions were needed. Three well repeats were set for each test, and the result was presented as the average values plus the standard derivations.

3. Result and Discussion

3.1. DCFH-1 Serves as an Excellent Fluorescence Substrate to HRP

Dichlorodihydrofluorescein carboxylic acid (DCFH) and its acetyl derivative DCFH-DA have been extensively applied in the detection of reactive oxygen species. DCFH is non-fluorescent, while strong fluorescence recovers upon the formation of the oxidized product DCF [32,33]. DCFHs is thus obtained by the reduction of DCFs. In this research, 2′,7′-dichlorofluorescein and its derivatives were used as the starting compounds to generate the corresponding **DCFH-1/2/3** through a mild reductive reaction (Figure 1a and the Supplementary Materials). A metal-free reduction reagent $NaBH_4/I_2$ was used to reduce the carbonyl group to prepare **DCFH-1** with a great isolated yield (80%) [34]. With the targeted DCFHs in hand, their reactivity towards HRP was examined. The carboxylic acid bearing product (**DCFH-2**) has been previously found as a good fluorescence indicator for HRP/H_2O_2 reaction [35,36]. As expected, obvious fluorescence enhancement from the **DCFH-2**/HRP/H_2O_2 reaction solution was observed in this research. However, both the final intensity and reaction rate are clearly lower than the reaction with **DCFH-1** as the substrate. Only a few minutes was required to reach an intensity plateau in terms of 50 nM HRP detection by **DCFH-1** (50 μM). In contrast, **DCFH-3** shows higher reactivity than **DCFH-2** but lower than **DCFH-1** (Figure 1b). The fluorescence spectra of all synthetic DCFHs reaction solutions peaked at around 520 nM, which indicated typical green emissions (Figure S1). The reaction solution with **DCFH-1** was then analyzed by HPLC, in which the chromatograph traces clearly indicated the generation of the oxidized product, which was further confirmed by HRMS (Figure S2). It was previously evidenced that fluorescein bearing a 2-carboxylic group or a 2-amide linkage on the axial benzene ring can form an equilibrium between a non-fluorescent lactone/lactam form and strong fluorescent ionic forms (Figure 1c) [37,38]. This equilibrium is mediated by proton transfer, which was affected by pHs, environmental hydrophobicity, and so on [39,40]. The benzyl alcohol group on **DCFH-1** is not a good proton donor due to its relatively higher pKa value. That might be one of the reasons to explain the differences between these synthetic DCFHs during HRP detection. However, the enzyme–substrate reactivity is not only affected by structural features of the substrate, but also mediated by other parameters, such as steric accessibility of the substrate to the catalytic center of the enzyme. In further studies, the stability and biocompatibility of **DCFH-1** were evaluated. As seen in Figure S3, **DCFH-1** has excellent stability in the dark, whereas continual exposure to room light can lead to the enhancement of background fluorescence. Similar to many other ROS probes, storage in the dark is also necessary for **DCFH-1**. Biocompatibility was examined using an in vitro cellular model; the result indicated low toxicity of HRP to the tested human hepatocellular carcinoma cell line (Huh-7) (Figure S4). Overall, **DCFH-1** holds great potential as a fluorescence turn-on substrate to HRP.

The commercially available substrate Amplex red is widely used to construct fluorescence ELISA kits and HRP-based multi-enzyme cascade kits for biochemical analysis. HRP catalyzed oxidation of Amplex red can generate a red-emitting product with the spectrum peak at around 586 nM in PBS buffer (Figure S5). In a further study, **DCFH-1** was directly compared with Amplex red in the sensing of the HRP/H_2O_2 reaction (Figure 2a). For **DCFH-1** and Amplex red assays, the fluorescence intensity at 528 nM (λ_{ex} = 504 nM) and 586 nM (λ_{ex} = 565 nM) was measured, respectively. As found in Figure 2b and Figure S6, the kinetic profiles indicated that both substrates exhibited signal enhancement upon reacting with HRP in obviously concentration-dependent manners. The pH effects on the reaction were then screened. The result indicates that **DCFH-1** works well under the pHs between 6.5 and 10.0 (Figure 3b), whereas Amplex red exhibits stable fluorescence signals under the pHs between 7.0 and 10.0 (Figure 3a). In comparison to the test with **DCFH-1**, a decreased concentration of HRP (10 nM) was applied for the Amplex red pH test, since higher concentrations of HRP can lead to an unexpected decrease in fluorescence upon a relatively long time reaction. More interestingly, the maximum intensity at the intensity plateau of the **DCFH-1**/HRP/H_2O_2 reaction is much greater than the maximum value of Amplex

red under the same reaction conditions. The fluorescence quantum yields of the targeted products upon HRP/H_2O_2 reaction were then calculated (Table S1 and Equation (S1)). As seen in Figure 2, the relative quantum yield (φ) of **DCFH-1** product is 0.83 in PBS (pH 7.4) buffers, while that for the Amplex red product resorufin is 0.20. The **DCFH-1** reaction product possesses higher quantum yield than that of Amplex red, which could explain the difference between the maximum intensities at the plateau of both substrates. The observation by the naked eye and by a smartphone camera also showed much brighter emission from **DCFH-1** than Amplex red upon sensing HRP/H_2O_2 (Figure S7). However, a relatively longer time was required for the **DCFH-1** reaction to reach its plateau when compared with Amplex red.

Next, HRP detection using **DCFH-1** was conducted by incubating **DCFH-1**/H_2O_2 in the presence of HRP at various concentrations, whose result was compared with the detection by Amplex red. Obvious HRP concentration-dependent fluorescence enhancement was observed for both substrates. There is an excellent linear relationship (R^2 = 0.991) between the fluorescence intensity and the HRP concentration when it ranges from 0.05 nM to 10 nM (Figure 4a). The linear relationship for Amplex red is found between 0.4 nM and 1.6 nM (Figure 4c). It is worth noting that the linear range of HRP detection by **DCFH-1** is much larger than those by Amplex red. The fluorescence intensity changes upon HRP sensing have also been characterized by the measurement of full fluorescence spectra (Figure 4b,d). The excitation wavelength was set at 450 nM and 520 nM for **DCFH-1** and Amplex red, respectively, in order to collect a full spectrum. Overall, the result indicates great application potential for **DCFH-1** to be used as a new fluorescence substrate to HRP.
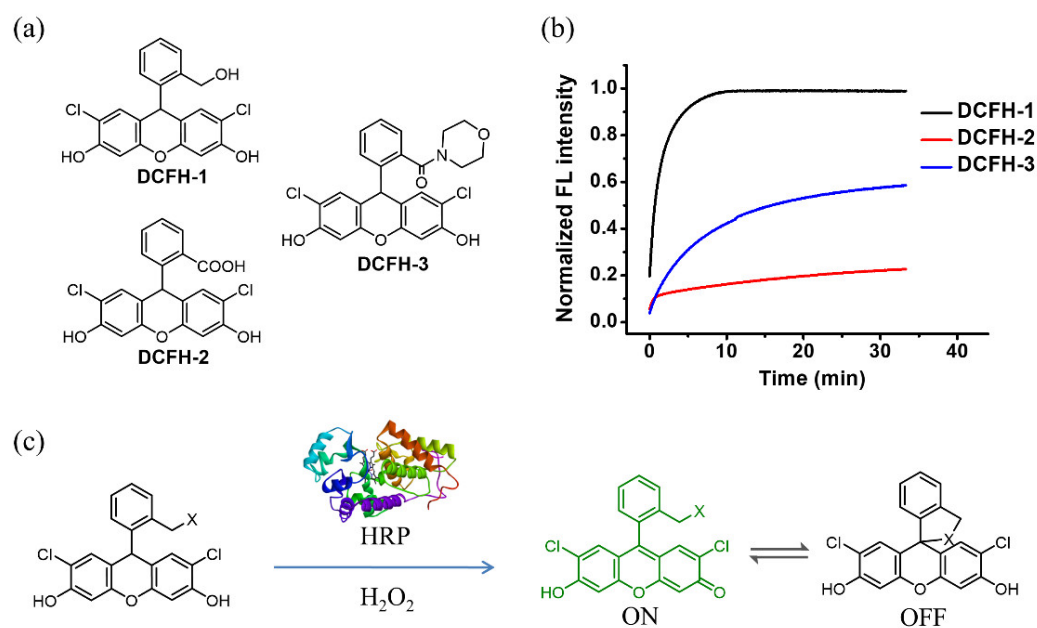

Figure 1. (**a**) The structures of the synthetic DCFHs. (**b**) Reaction kinetic curves by monitoring the fluorescence of the reaction solution, the maximum intensity was normalized to 1 for easier comparison. (**c**) Schematic Figure Shows the HRP catalyzed reaction on DCFHs.
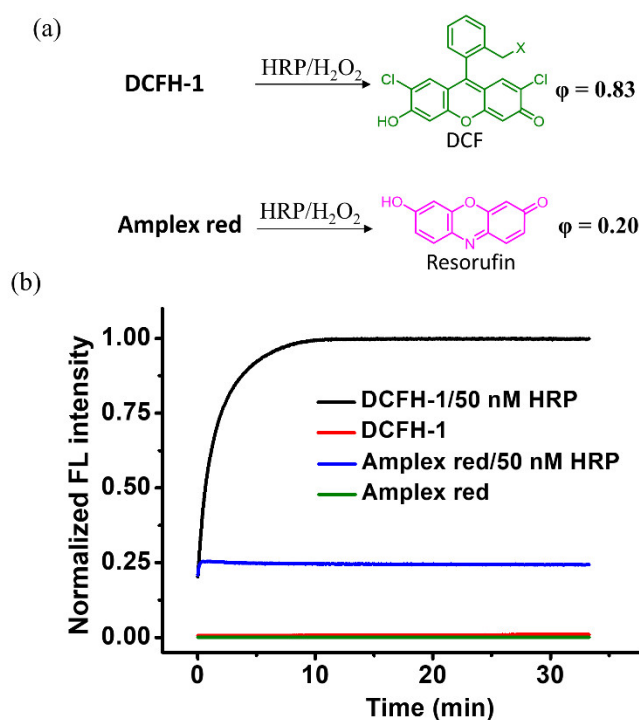
(a)

DCFH-1 $\xrightarrow{\text{HRP/H}_2\text{O}_2}$ DCF $\varphi = 0.83$

Amplex red $\xrightarrow{\text{HRP/H}_2\text{O}_2}$ Resorufin $\varphi = 0.20$

(b)

Figure 2. (**a**) The reaction and the corresponding fluorescent products generated in the substrate/HRP reaction systems. (**b**) Kinetic response curves of **DCFH-1** and Amplex red upon reaction with HRP (50 nM and 0 nM), respectively, in the presence of excess amount H_2O_2. The maximum intensity was normalized to 1 for easier comparison.
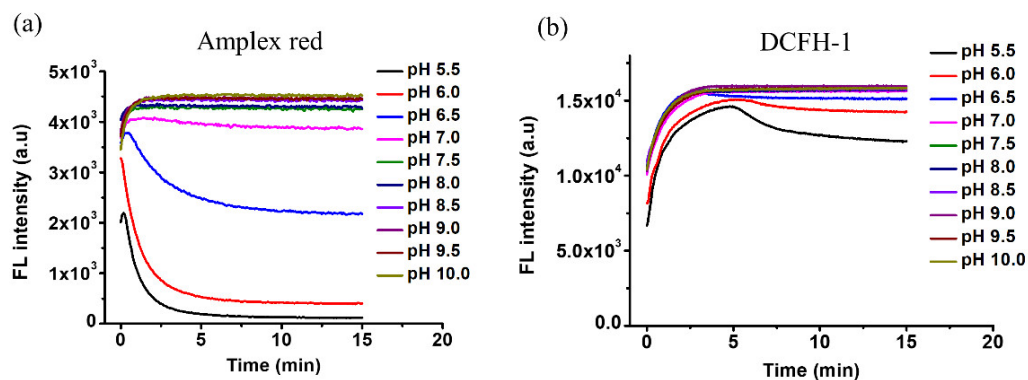

Figure 3. (**a**) The response kinetic curves of Amplex red upon reaction with HRP/H_2O_2 under different pH conditions, where the final concentrations in the reaction mixture of the Amplex red, HRP, and H_2O_2 were set at 50 μM, 10 nM, and 10 mM, respectively. (**b**) pH effects on the detection by **DCFH-1**, where the concentrations of **DCFH-1**, HRP, and H_2O_2 were set at 50 μM, 50 nM, and 10 mM, respectively. The 1× PBS (10 mM) solutions were adjusted by 2 M NaOH and/or 2 M HCl to make the solutions with various pHs.

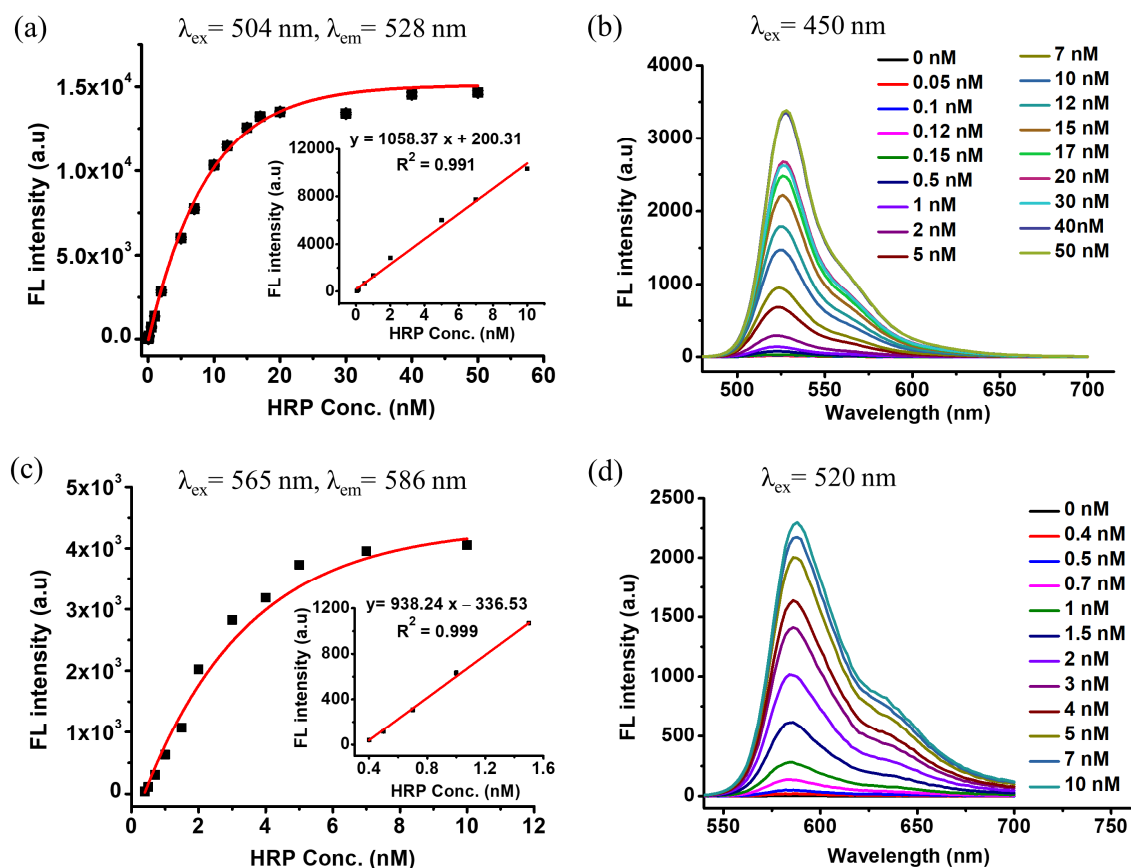**Figure 4.** (**a**) The detection curve of **DCFH-1** in the presence of series concentrations of HRP; the insert stands for a linear relationship between the intensity and HRP concentration. (**b**) Full fluorescence spectra of **DCFH-1** reaction solution upon HRP detection, which was excited at 450 nM. (**c**) The detection curve of Amplex red in the presence of series concentrations of HRP; the insert stands for a linear relationship between the intensity and HRP concentration. (**d**) Full fluorescence spectra of Amplex red reaction solution upon HRP detection, which was excited at 520 nM.

3.2. Nonspecific Esterase Reactivity of DCFH-1 and Amplex Red

It has been previously pointed out that Amplex red can respond to carboxylesterase through fluorescence turn-on, which leads to inaccuracy in analytical practices. The mechanism can be explained as follows: carboxylesterase can remove the acetyl group on Amplex red, and the residue is then oxidized by the molecular oxygen in the air to generate the fluorescent resorufin [19]. In contrast, **DCFH-1** does not have any ester or amide bond that might become the substrate of carboxylesterase, whose fluorescence would not be affected by carboxylesterase. To prove this, carboxylesterase was mixed with **DCFH-1** and Amplex red, respectively (Figure 5a). As shown in Figure 5b, the Amplex red/esterase solution indeed indicated a fluorescence increase as the incubation time increased. Over 100-fold fluorescence enhancement was observed after 20 min incubation, whereas incubation with esterase did not lead to fluorescence changes in the solution of **DCFH-1** (Figure 5b). PMSF is a well-known protease inhibitor that also has inhibition activity toward carboxylesterase. As indicated in Figure 5, upon inhibition by PMSF, the fluorescence turn-on from Amplex red/esterase was suppressed completely. The reaction solution of PMSF/**DCFH-1**/esterase does not result in fluorescence turn-on, which shows a similar trend to **DCFH-1**/esterase.
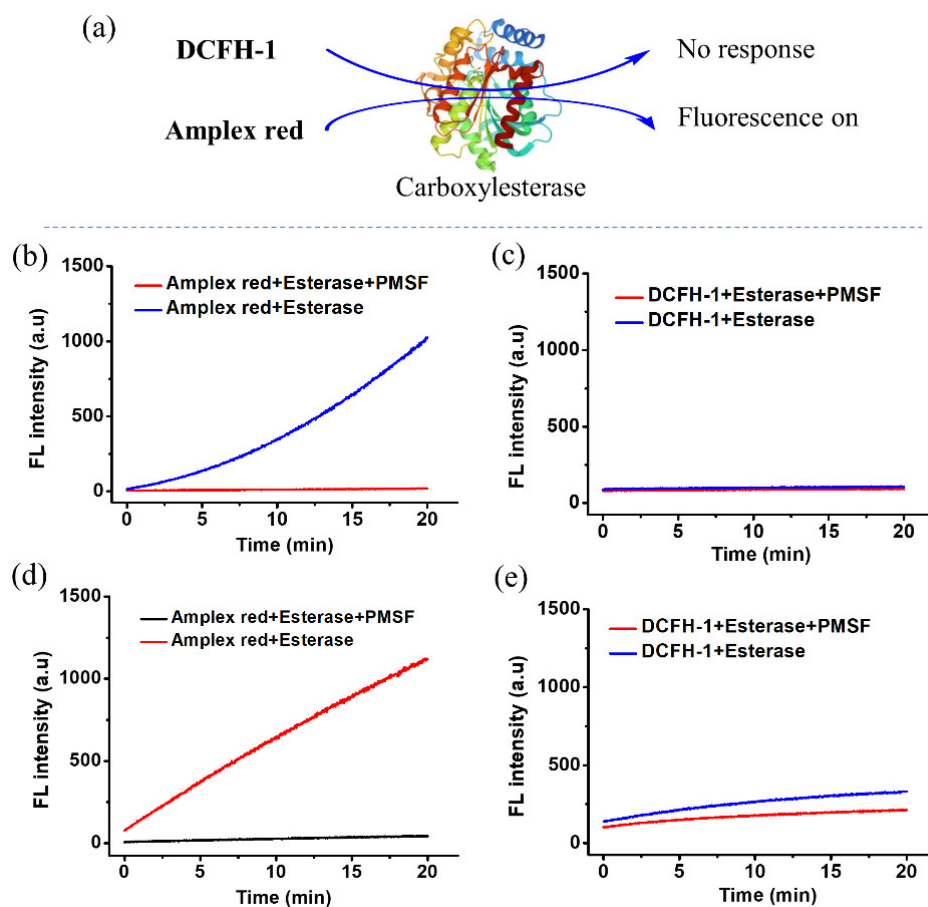
Figure 5. (**a**) Schematic Figure Shows nonspecific responsiveness of Amplex red and **DCFH-1** toward carboxylesterase; (**b**,**c**) the kinetic fluorescence responses of Amplex red and **DCFH-1** upon incubation with the commercialized pure enzyme; and (**d**,**e**) the kinetic fluorescence responses of Amplex red and **DCFH-1** upon incubation with the protein extracts from the mouse liver tissues. PMSF was applied as an inhibitor to carboxylesterase.

In parallel, the nonspecific esterase reactivity was also tested by incubating the substrates with the protein extracts of fresh mouse liver tissues. PMSF was also used to inhibit the activity of carboxylesterase in the tissue extracts. Figure 5d shows that fluorescence turn-on from Amplex red occurs upon the incubation with the tissue extracts; PMSF can almost completely suppress the fluorescence response. Fluorescence enhancement of **DCFH-1** was observed unexpectedly when incubating with the tissue extracts, where PMSF led to a slight inhibition of the fluorescence response (Figure 5e). It is worth noting that the fluorescence intensities of the **DCFH-1** solution both in the absence and in the presence of PMSF are obviously lower than those from Amplex red. The fluorescence changes of **DCFH-1** are mostly due to the oxidative reaction led by the reactive oxygen species (ROS) and reactive nitrogen species (RNS) in the fresh tissue extracts. In fact, the carboxylic group bearing DCFH (**DCFH-2**) has previously been used as ROS and RNS probes, which could explain the similar reactivity on **DCFH-1**.

3.3. Fluorescence ELISA Using DCFH-1

DCFH-1 exhibited an excellent fluorescence response to the HRP/H_2O_2 reaction, thus holding great potential in HRP-based immunoassays such as ELISA. For the proof of concept, the detection reagent in the commercial ELISA kit was replaced with **DCFH-1** solution to establish an alternated ELISA kit. Two cytokines, TNF-α and IL-6, in the culture mediums of the mouse macrophage-like cell line RAW264.7 were quantified by the **DCFH-1**-modified ELISA kit. Before the measurement, standard calibration curves

using the **DCFH-1** ELISA kit were prepared. As shown in Figure 6, the linear calibration curve for TNF-α was found between the concentrations from 0 to 2000 pg/mL, and that for IL-6 was found between 0 and 500 pg/mL. It is worth noting that the coefficient of determination R^2 for both detections are all over 0.99. The above result indicates that **DCFH-1** is an excellent HRP substrate for ELISA. It is known that the bacterial endotoxin LPS has been extensively used to stimulate RAW264.7 cells for establishing cellular models of inflammation. The elevated release of cytokines, including TNF-α and IL-6, as well as the gaseous signaling molecule nitric oxide (NO), are regarded to be associated with the development of inflammation [41,42]. As seen in Figure 6, both TNF-α and IL-6 from the real biological samples were successfully measured by **DCFH-1** ELISA. As expected, treatment with LPS at nanogram levels can significantly increase the amount of TNF-α and IL-6 in cell culture media. In parallel, NO was quantified by a standard Griess assay [43]. As indicated by Figure S8, LPS at nanogram levels can also significantly elevate NO release from RAW264.7 cells, which possess a similar trend to the result of TNF-α and IL-6 quantification. Overall, it is obvious that ELISA kits with **DCFH-1** as the fluorescence indicator have great application prospects in HRP-based immunoassays.
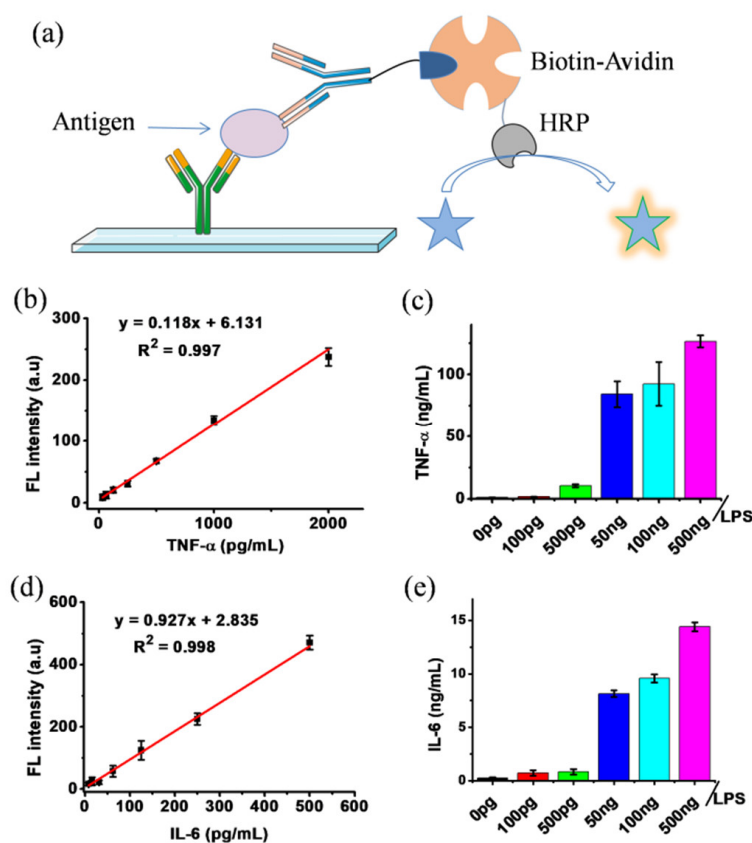

Figure 6. (**a**) Schematic figure illustrates the fluorescence detection procedure using **DCFH-1** alternated ELISA kit. (**b**) The standard calibration curve obtained by using **DCFH-1** as the fluorescence indicator in TNF-α detection. (**c**) TNF-α quantification result from the culture medium of inflammatory cell model. (**d**) The standard calibration curve obtained by using **DCFH-1** as the fluorescence indicator in IL-6 detection. (**e**) IL-6 quantification result from the cultural medium of inflammatory cell model. LPS was used to stimulate the RAW264.7 cells to release more cytokines.

4. Conclusions

Three dihydofluorescein analogues (DCFHs) were prepared, characterized and tested as fluorescence substrates to the most widely used enzyme, HRP, in immunoassays. The most promising, **DCFH-1,** exhibited excellent responsiveness toward HRP/H_2O_2 reaction. Importantly, **DCFH-1** shows comparable sensitivity in sensing HRP and a relatively larger

linear detection range than the commercial HRP substrate, Amplex red. In addition, **DCFH-1** does not respond to carboxylesterase, thus can overcome the nonspecific issue that occurs with Amplex red. In real immunoassays, the **DCFH-1** ELISA kit works very well in the determination of the cytokines TNF-α and IL-6 from mouse macrophages. It is worth stressing that **DCFH-1** is easily obtained through a single-step synthetic procedure with a high isolated yield. Overall, **DCFH-1** can serve as an excellent fluorescence substrate to HRP, which will have great application prospects in HRP-based biochemical analysis.

Supplementary Materials: The following supporting information can be downloaded at: https://www.mdpi.com/article/10.3390/chemosensors11020152/s1, Figure S1: UV–vis absorbance spectra (a) and fluorescence spectra (b) of the synthetic DCFHs upon reaction with HRP/H_2O_2. Figure S2: HPLC analysis of the product formation from the **DCFH-1**/HRP/H_2O_2 reaction solution. Figure S3: The fluorescence spectra changes from **DCFH-1** solutions upon storing in the dark (a) and with exposure to room light (b). Figure S4: Cell viability result upon incubation with **DCFH-1** at different concentrations. Figure S5: UV–vis absorbance spectrum (a) and fluorescence spectrum (b) of Amplex red upon reaction with HRP/H_2O_2. The maximum intensity was normalized to 1 for easier comparison. Figure S6: (a) The response kinetic curves of Amplex red upon reaction with HRP/H_2O_2 under different pH conditions. (b) pH effects on the detection by **DCFH-1**. Figure S7: Fluorescence images of the detection solutions by **DCFH-1** (green color) and Amplex red (red color). The figure was captured by a smartphone camera. Figure S8: NO quantification from the cell culture medium [43]. The sample was diluted to match the detection range in case needed. Figures S9–S16: nMR spectra of the synthetic compounds. Equation (S1): the function for the calculation of relative fluorescence quantum yields [44,45]. Table S1: The parameters for relative quantum yield calculation.

Author Contributions: Conceptualization and funding acquisition, F.L., T.D. and Y.Z.; methodology and investigation, J.Z., T.L., S.Z. and X.Z.; review and editing, W.L. and Z.L. All authors have read and agreed to the published version of the manuscript.

Institutional Review Board Statement: The protocol for use of mouse liver tissues was approved by the Animal Ethics Committee of Guangzhou University of Chinese Medicine (PZ22047), which is in accordance with the national regulatory principles.

Conflicts of Interest: The authors declare no conflict of interest.

References

1. Gorris, H.H.; Walt, D.R. Mechanistic aspects of horseradish peroxidase elucidated through single-molecule studies. *J. Am. Chem. Soc.* **2009**, *131*, 6277–6282. [CrossRef]
2. Azevedo, A.M.; Martins, V.C.; Prazeres, D.M.; Vojinović, V.; Cabral, J.M.; Fonseca, L.P. Horseradish peroxidase: A valuable tool in biotechnology. *Biotechnol. Annu. Rev.* **2003**, *9*, 199–247. [CrossRef]
3. Sellami, K.; Couvert, A.; Nasrallah, N.; Maachi, R.; Abouseoud, M.; Amrane, A. Peroxidase enzymes as green catalysts for bioremediation and biotechnological applications: A review. *Sci. Total Environ.* **2022**, *806*, 150500. [CrossRef]
4. Lin, L.; Yi, Z.; Liang, S.; Yongxin, L.; Wei, H.; Mengda, C.; Naidi, Y.; Qiong, W.; Zhongxi, H.; Changmin, Y.; et al. Ultrasensitive detection of IgE levels based on magnetic nanocapturer linked immunosensor assay for early diagnosis of cancer. *Chin. Chem. Lett.* **2022**, *33*, 1855–1860. [CrossRef]
5. Liu, G.; Wang, L.; Zhu, F.; Liu, Q.; Feng, Y.; Zhao, X.; Chen, M.; Chen, X. Facile construction of a reusable multi-enzyme cascade bioreactor for effective fluorescence discrimination and quantitation of amino acid enantiomers. *Chem. Eng. J.* **2022**, *428*, 131975. [CrossRef]
6. Faqin, D.; Jin, L.; Yevgeny, A.G.; Shiyong, S.; Yan, L.; Rui, L.; Ke, W.; Daoyong, T.; Olga, B.K.; Xiaoqin, N. High-performance cascade nanoreactor based on halloysite nanotubes-integrated enzyme-nanozyme microsystem. *Chin. Chem. Lett.* **2022**, *33*, 807–811. [CrossRef]
7. Li, M.; Su, H.; Tu, Y.; Shang, Y.; Liu, Y.; Peng, C.; Liu, H. Development and Application of an Efficient Medium for Chromogenic Catalysis of Tetramethylbenzidine with Horseradish Peroxidase. *ACS Omega* **2019**, *4*, 5459–5470. [CrossRef]

8. Li, F.; Zhang, Y.; Liu, J.; He, J. Luminol, horseradish peroxidase and antibody ternary codified gold nanoparticles for a label-free homogenous chemiluminescent immunoassay. *Anal. Methods* **2018**, *10*, 722–729. [CrossRef]

9. Wang, N.; Miller, C.J.; Wang, P.; Waite, T.D. Quantitative determination of trace hydrogen peroxide in the presence of sulfide using the Amplex Red/horseradish peroxidase assay. *Anal. Chim. Acta* **2017**, *963*, 61–67. [CrossRef]

10. Taylor, S.C.; Rosselli-Murai, L.K.; Crobeddu, B.; Plante, I. A critical path to producing high quality, reproducible data from quantitative western blot experiments. *Sci. Rep.* **2022**, *12*, 17599. [CrossRef]

11. Karatani, H. Luminol–hydrogen peroxide–horseradish peroxidase chemiluminescence intensification by kosmotrope ammonium sulfate. *Anal. Sci.* **2022**, *38*, 613–621. [CrossRef]

12. Ye, Q.; Ren, S.; Huang, H.; Duan, G.; Liu, K.; Liu, J.-B. Fluorescent and Colorimetric Sensors Based on the Oxidation of o-Phenylenediamine. *ACS Omega* **2020**, *5*, 20698–20706. [CrossRef]

13. Wang, Y.; Hu, H.; Dong, T.; Mansour, H.; Zhang, X.; Li, F.; Wu, P. Double-Stranded DNA Matrix for Photosensitization Switching. *CCS Chem.* **2021**, *3*, 2394–2404. [CrossRef]

14. Chen, Y.; Yang, X.; Lu, C.; Yang, Z.; Wu, W.; Wang, X. Novel colorimetric, photothermal and up-conversion fluorescence triple-signal sensor for rosmarinic acid detection. *Chin. Chem. Lett.* **2022**, 108099. [CrossRef]

15. Zhang, X.; Li, C.; Zhang, Y.; Guan, X.; Mei, L.; Feng, H.; Li, J.; Tu, L.; Feng, G.; Deng, G.; et al. Construction of Long-Wavelength Emissive Organic Nanosonosensitizer Targeting Mitochondria for Precise and Efficient In Vivo Sonotherapy. *Adv. Funct. Mater.* **2022**, *32*, 2207259. [CrossRef]

16. Li, K.; Ren, T.-B.; Huan, S.; Yuan, L.; Zhang, X.-B. Progress and Perspective of Solid-State Organic Fluorophores for Biomedical Applications. *J. Am. Chem. Soc.* **2021**, *143*, 21143–21160. [CrossRef]

17. Sun, Z.; Zhao, L.; Li, C.; Jiang, Y.; Wang, F. Direct Z-scheme In2S3/Bi2S3 heterojunction-based photoelectrochemical aptasensor for detecting oxytetracycline in water. *J. Environ. Chem. Eng.* **2022**, *10*, 107404. [CrossRef]

18. Serrano, J.; Jové, M.; Boada, J.; Bellmunt, M.J.; Pamplona, R.; Portero-Otín, M. Dietary antioxidants interfere with Amplex Red-coupled-fluorescence assays. *Biochem. Biophys. Res. Commun.* **2009**, *388*, 443–449. [CrossRef]

19. Miwa, S.; Treumann, A.; Bell, A.; Vistoli, G.; Nelson, G.; Hay, S.; von Zglinicki, T. Carboxylesterase converts Amplex red to resorufin: Implications for mitochondrial H2O2 release assays. *Free Radical Biol. Med.* **2016**, *90*, 173–183. [CrossRef]

20. Wang, T.; Xiang, Y.; Liu, X.; Chen, W.; Hu, Y. A novel fluorimetric method for laccase activities measurement using Amplex Red as substrate. *Talanta* **2017**, *162*, 143–150. [CrossRef]

21. Zhao, B.; Ranguelova, K.; Jiang, J.; Mason, R.P. Studies on the photosensitized reduction of resorufin and implications for the detection of oxidative stress with Amplex Red. *Free Radical Biol. Med.* **2011**, *51*, 153–159. [CrossRef]

22. Shatsauskas, A.; Shatalin, Y.; Shubina, V.; Zablodskii, Y.; Chernenko, S.; Samsonenko, A.; Kostyuchenko, A.; Fisyuk, A. Synthesis and application of new 3-amino-2-pyridone based luminescent dyes for ELISA. *Dyes Pigm.* **2021**, *187*, 109072. [CrossRef]

23. Liu, Z.; Wang, X.; Ren, X.; Li, W.; Sun, J.; Wang, X.; Huang, Y.; Guo, Y.; Zeng, H. Novel fluorescence immunoassay for the detection of zearalenone using HRP-mediated fluorescence quenching of gold-silver bimetallic nanoclusters. *Food Chem.* **2021**, *355*, 129633. [CrossRef]

24. Sun, J.; Zhao, J.; Wang, L.; Li, H.; Yang, F.; Yang, X. Inner Filter Effect-Based Sensor for Horseradish Peroxidase and Its Application to Fluorescence Immunoassay. *ACS Sens.* **2018**, *3*, 183–190. [CrossRef]

25. Acharya, A.P.; Sen, P.; Aran, K.; Gardner, A.B.; Rafi, M.; Dean, D.; Murthy, N. A turn-off fluorescent substrate for horseradish peroxidase improves the sensitivity of ELISAs. *J. Polym. Sci. Part A Polym. Chem.* **2015**, *53*, 206–210. [CrossRef]

26. Wu, M.; Wong, G.T.F.; Wu, Y.C. The Scopoletin-HRP Fluorimetric Determination of H(2)O(2) in Seawaters-A Plea for the Two-Stage Protocol. *Methods Protoc.* **2017**, *1*, 4. [CrossRef]

27. Liu, J.; Ruan, G.; Ma, W.; Sun, Y.; Yu, H.; Xu, Z.; Yu, C.; Li, H.; Zhang, C.-w.; Li, L. Horseradish peroxidase-triggered direct in situ fluorescent immunoassay platform for sensing cardiac troponin I and SARS-CoV-2 nucleocapsid protein in serum. *Biosens. Bioelectron.* **2022**, *198*, 113823. [CrossRef]

28. Chen, X.-L.; Li, D.-H.; Yang, H.-H.; Zhu, Q.-Z.; Zheng, H.; Xu, J.-G. Study of tetra-substituted amino aluminum phthalocyanine as a new red-region substrate for the fluorometric determination of peroxidase and hydrogen peroxide. *Anal. Chim. Acta* **2001**, *434*, 51–58. [CrossRef]

29. Khosravi, M.; Nouri, M.; Mohammadi, A.; Mosavari, N.; Constable, P.D. Preparation of immunomagnetic beads coupled with a rhodamine hydrazine immunosensor for the detection of Mycobacterium avium subspecies paratuberculosis in bovine feces, milk, and colostrum. *J. Dairy Sci.* **2021**, *104*, 6944–6960. [CrossRef]

30. Acharya, A.P.; Nafisi, P.M.; Gardner, A.; Mackay, J.L.; Kundu, K.; Kumar, S.; Murthy, N. A fluorescent peroxidase probe increases the sensitivity of commercial ELISAs by two orders of magnitude. *Chem. Commun.* **2013**, *49*, 10379–10381. [CrossRef]

31. Yoo, S.; Kim, S.; Jeon, S.; Han, M.S. Aldehyde N,N-dimethylhydrazone-based fluorescent substrate for peroxidase-mediated assays. *RSC Adv.* **2022**, *12*, 8668–8673. [CrossRef]

32. Reiniers, M.J.; van Golen, R.F.; Bonnet, S.; Broekgaarden, M.; van Gulik, T.M.; Egmond, M.R.; Heger, M. Preparation and Practical Applications of 2′,7′-Dichlorodihydrofluorescein in Redox Assays. *Anal. Chem.* **2017**, *89*, 3853–3857. [CrossRef]

33. Deng, T.; Bao, H.; Huang, W.; Wang, X.; Hu, S.; Wu, S.; Zhao, L.; Cai, C.; Hu, Y.; Liu, F. Easy access of dihydrofluoresceins as advanced fluorescence turn-on probes for oxidative stress. *Dyes Pigm.* **2020**, *173*, 107915. [CrossRef]

34. Haldar, P.; Barman, G.; Ray, J.K. Sodium borohydride–iodine mediated reduction of γ-lactam carboxylic acids followed by DDQ mediated oxidative aromatisation: A simple approach towards N-aryl-formylpyrroles and 1,3-diaryl-formylpyrroles. *Tetrahedron* **2007**, *63*, 3049–3056. [CrossRef]

35. Kessler, A.; Hedberg, J.; McCarrick, S.; Karlsson, H.L.; Blomberg, E.; Odnevall, I. Adsorption of Horseradish Peroxidase on Metallic Nanoparticles: Effects on Reactive Oxygen Species Detection Using 2′,7′-Dichlorofluorescin Diacetate. *Chem. Res. Toxicol.* **2021**, *34*, 1481–1495. [CrossRef]

36. Ghéczy, N.; Sasaki, K.; Yoshimoto, M.; Pour-Esmaeil, S.; Kröger, M.; Stano, P.; Walde, P. A two-enzyme cascade reaction consisting of two reaction pathways. Studies in bulk solution for understanding the performance of a flow-through device with immobilised enzymes. *RSC Adv.* **2020**, *10*, 18655–18676. [CrossRef]

37. Le Guern, F.; Mussard, V.; Gaucher, A.; Rottman, M.; Prim, D. Fluorescein Derivatives as Fluorescent Probes for pH Monitoring along Recent Biological Applications. *Int. J. Mol. Sci.* **2020**, *21*, 9217. [CrossRef]

38. Klonis, N.; Sawyer, W.H. Spectral properties of the prototropic forms of fluorescein in aqueous solution. *J. Fluoresc.* **1996**, *6*, 147–157. [CrossRef]

39. Keller, S.; Kamiya, M.; Urano, Y. Recent Progress in Small Spirocyclic, Xanthene-Based Fluorescent Probes. *Molecules* **2020**, *25*, 5964. [CrossRef]

40. Turnbull, J.L.; Benlian, B.R.; Golden, R.P.; Miller, E.W. Phosphonofluoresceins: Synthesis, Spectroscopy, and Applications. *J. Am. Chem. Soc.* **2021**, *143*, 6194–6201. [CrossRef]

41. Facchin, B.M.; Dos Reis, G.O.; Vieira, G.N.; Mohr, E.T.B.; da Rosa, J.S.; Kretzer, I.F.; Demarchi, I.G.; Dalmarco, E.M. Inflammatory biomarkers on an LPS-induced RAW 264.7 cell model: A systematic review and meta-analysis. *Inflamm. Res.* **2022**, *71*, 741–758. [CrossRef]

42. He, L.; He, L.-H.; Xu, S.; Ren, T.-B.; Zhang, X.-X.; Qin, Z.-J.; Zhang, X.-B.; Yuan, L. Engineering of Reversible NIR-II Redox-Responsive Fluorescent Probes for Imaging of Inflammation In Vivo. *Angew. Chem. Int. Ed.* **2022**, *61*, e202211409. [CrossRef]

43. Deng, T.; Hu, S.; Huang, X.-a.; Song, J.; Xu, Q.; Wang, Y.; Liu, F. A novel strategy for colorimetric detection of hydroxyl radicals based on a modified Griess test. *Talanta* **2019**, *195*, 152–157. [CrossRef]

44. Brouwer, A.M. Standards for photoluminescence quantum yield measurements in solution (IUPAC Technical Report). *Pure Appl. Chem.* **2011**, *83*, 2213–2228. [CrossRef]

45. Deng, T.; Wang, X.; Wu, S.; Hu, S.; Liu, W.; Chen, T.; Yu, Z.; Xu, Q.; Liu, F. A new FRET probe for ratiometric fluorescence detecting mitochondria-localized drug activation and imaging endogenous hydroxyl radicals in zebrafish. *Chem. Commun.* **2020**, *56*, 4432–4435. [CrossRef]